Eur. Phys. J. C (2022) 82:1053
https://doi.org/10.1140/epjc/s10052-022-11028-y

THE EUROPEAN PHYSICAL JOURNAL C

Regular Article - Theoretical Physics

Scrutinizing the 95–100 GeV di-tau excess in the top associated process

Syuhei Iguro[1,2,a], **Teppei Kitahara**[3,4,5,b], **Yuji Omura**[6,c]

[1] Institute for Theoretical Particle Physics (TTP), Karlsruhe Institute of Technology (KIT), Engesserstraße 7, 76131 Karlsruhe, Germany
[2] Institute for Astroparticle Physics (IAP), KIT, Hermann-von-Helmholtz-Platz 1, 76344 Eggenstein-Leopoldshafen, Germany
[3] Institute for Advanced Research, Nagoya University, Nagoya 464-8601, Japan
[4] Kobayashi-Maskawa Institute for the Origin of Particles and the Universe, Nagoya University, Nagoya 464-8602, Japan
[5] Theory Center, IPNS, High Energy Accelerator Research Organization (KEK), 1-1 Oho, Tsukuba 305-0801, Japan
[6] Department of Physics, Kindai University, Higashi-Osaka, Osaka 577-8502, Japan

Received: 16 May 2022 / Accepted: 12 November 2022

Abstract Recently, the CMS collaboration has reported a di-tau excess with a local significance of 2.6–3.1σ where the invariant mass is $m_{\tau\tau} = 95$–$100\,\text{GeV}$. This excess can be interpreted as a light scalar boson that couples to the third generation fermions, particularly top and τ. Based on the simplest model that can account for the CMS di-tau excess, we evaluate experimental sensitivities to the additional light resonance, using the results reported by the ATLAS collaboration. We see that a search for the top-quark associated production of the SM Higgs boson that decays into $\tau\bar{\tau}$ sets a strong model-independent limit. We also find that the CP-even scalar interpretation of the light resonance is excluded by the ATLAS results, while the CP-odd interpretation is not.

Contents

1 Introduction

The Standard Model (SM) has been experimentally verified with high accuracy and very successful. In the SM, the Higgs field plays a role in the mass generation of particles. The potential for the Higgs field is given to break the electroweak (EW) symmetry, and particle masses are originated from the non-vanishing vacuum expectation value (VEV). This mechanism has been tested by the EW precision observables, the 125-GeV Higgs measurements, and so on, and the predictions correspond reasonably well with the experimental results. This success, however, poses a question about the origin of the Higgs potential. In particular, the mass squared of the Higgs field is negative and requires a severe fine-tuning to cancel the very large radiative corrections. In order to avoid the fine-tuning, many models beyond the SM have been proposed so far; e.g., supersymmetry, composite Higgs, little Higgs, top partner, extra dimensions, and gauge-Higgs unification. These extended models generally predict additional particles around TeV scale, that can be tested in the experiments at the large hadron collider (LHC). Among the new particles, additional scalar fields are often suggested as good candidates to validate the models. The additional scalars, therefore, have been studied widely in both model-dependent and model-independent ways.

Interestingly, such a new particle, that interacts with the SM particles through the weak interaction and/or Yukawa interactions, can still take mass of $\mathcal{O}(100)\,\text{GeV}$ [1,2], if the couplings with light quarks and leptons are suppressed. The possibility of an additional scalar boson lighter than the 125 GeV Higgs still remains. Recently, the CMS collaboration has reported a new excess in the di-tau final states

[a] e-mail: igurosyuhei@gmail.com
[b] e-mail: teppeik@kmi.nagoya-u.ac.jp (corresponding author)
[c] e-mail: yomura@phys.kindai.ac.jp

Published online: 21 November 2022

within all the τ decay modes (leptonic and hadronic) by using the Run 2 full data [3], which is an extension of the previous searches [4–9]. The excess can be interpreted as a resonance of a new particle. The local and global significance of the excess are 2.6σ and 2.3σ at the invariant mass of $m_{\tau\tau} = 95\,\text{GeV}$, respectively.[1] At $m_{\tau\tau} = 100\,\text{GeV}$, these values are 3.1σ and 2.7σ. By introducing an additional single neutral narrow resonance ϕ, the best fit values for the excess are [3]

$$\sigma(gg \to \phi) \times \text{BR}(\phi \to \tau\bar{\tau}) = 7.7^{+3.9}_{-3.1}\,\text{pb} \quad \text{for } m_\phi = 95\,\text{GeV}, \tag{1}$$

or

$$\sigma(gg \to \phi) \times \text{BR}(\phi \to \tau\bar{\tau}) = 5.8^{+2.4}_{-2.0}\,\text{pb} \quad \text{for } m_\phi = 100\,\text{GeV}. \tag{2}$$

These cross sections are comparable to the 125 GeV SM Higgs boson, h [11],

$$\sigma(gg \to h) \times \text{BR}(h \to \tau\bar{\tau}) = 3.1 \pm 0.2\,\text{pb}. \tag{3}$$

Note that there is no excess in the b-tagging category, which implies that the b-associated ϕ production is disfavored.

Interestingly, in the same mass region, a different excess has also been reported in the di-photon final states by the CMS collaboration based on the full Run 1 [12] and the first Run 2 ($35.9\,\text{fb}^{-1}$) data [13]. The local and global significance are 2.8σ and 1.3σ at $m_{\gamma\gamma} = 95.3\,\text{GeV}$. This excess can be interpreted as a new resonance, ϕ, that decays to two photons, i.e., $gg \to \phi \to \gamma\gamma$ (see Eq. (31)). Although the similar analysis has been performed by the ATLAS collaboration [14], the sensitivity is not good enough to check the consistency [15]. Moreover, another mild excess has been reported in the LEP experiment, that can be interpreted as $e^+e^+ \to Z\phi \to Zb\bar{b}$ [16]. The signal corresponds to 2.3σ local significance at $m_\phi = 98\,\text{GeV}$. Therefore, it is very interesting to consider the possibility that these excesses are caused by the same new particle ϕ. A variety of new physics interpretations have been discussed in Refs. [17–32] focusing on the CMS di-photon and the LEP $b\bar{b}$ excesses, while in Refs. [33,34] including the CMS di-tau excess as well.

In this paper, we point out that associated production of ϕ with two top quarks can provide a simple and powerful way to verify the di-tau excess in Eqs. (1) and (2). In Fig. 1, the relevant diagrams for $gg \to \tau\bar{\tau}$ and $gg \to t\bar{t} + \tau\bar{\tau}$ are shown. As shown Eq. (3), the di-tau excess requires the new resonance cross section almost comparable to the SM Higgs boson via the gluon fusion. The $\tau\bar{\tau}$ resonance at 95–100 GeV, however, suffers from the huge Z boson background which stems from the tree-level Drell–Yan (DY) process. Such a Z peak pollution will be mild when the top-quark associated production is selected. This is because that the production cross section of $t\bar{t} + Z$ and $t\bar{t} + h$ are the same size in the SM (see Sect. 2.1 for the explicit numbers), and furthermore, the new resonance is produced by the tree level, which could amplify the sensitivity to probe the new resonance. We will investigate the LHC sensitivity to the possible 95–100 GeV resonance in the top-associated process.

In Sect. 2, we introduce the minimal setup to account for the $\tau\bar{\tau}$ excess and summarize the predictions of the top-associated productions. In Sect. 3, the numerical analysis to derive the upper limits on the model-independent $t\bar{t} + \tau\bar{\tau}$ cross section is performed for the new resonance. Section 4 is devoted to summary and discussion.

2 Setup

In this section, we introduce a simplified model that can account for the excesses in the 95–100 GeV region. We introduce an additional scalar boson which has large couplings with top and τ, since the gluon fusion is dominated by the chiral heavy fermion loop [35] and the resonance preferentially decays into τ leptons. It is noted that no excess is found with $\tau\bar{\tau}$ resonant events in association with b quark jets [3], so that a coupling with b is unlikely to be large. There are several ways to derive such a scalar effectively at low energy. In this study, we do not specify models and simply assume that extra neutral scalars, H and A, couple to top and τ as follows:

$$-\mathcal{L}_{\text{eff}} = \frac{\rho^H_{tt}}{\sqrt{2}}\,\bar{t}Ht + \frac{\rho^H_{\tau\tau}}{\sqrt{2}}\,\bar{\tau}H\tau \pm i\frac{\rho^A_{tt}}{\sqrt{2}}\,\bar{t}A\gamma_5 t + i\frac{\rho^A_{\tau\tau}}{\sqrt{2}}\,\bar{\tau}A\gamma_5\tau. \tag{4}$$

The all couplings, ρ^ϕ_{tt} and $\rho^\phi_{\tau\tau}$ ($\phi = H, A$), are real in our study. Then, H (A) corresponds to a CP-even (CP-odd) scalar.[2] As we will see, the γ_5 structure plays an important role in our analysis. Note that the relative sign for the A interaction depends on the UV theory. In our study, this relative sign does not affect the conclusion.

The possible UV completion of the light scalar boson could be the Two-Higgs-Doublet Model (2HDM) with a real singlet scalar [23,27,29,30,33,34], flavor-aligned 2HDM

[1] They have also reported a 2.8σ (local) and 2.4σ (global) excess at $m_{\tau\tau} = 1.2\,\text{TeV}$. It is, however, excluded by the same search by the ATLAS collaboration [10].

[2] Although additional vector particle, that couples to the top and τ [36], could also be considered as the candidate, the gluon fusion (via the top loop) vanishes for the vector boson production when the fermion interactions are vector couplings [37]. We will discuss the possibility of the vector particle interpretation in Sect. 4.

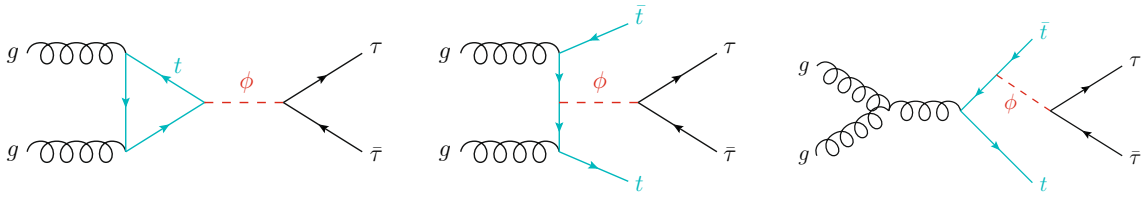

Fig. 1 Representative Feynman diagrams for a narrow resonance ϕ exchange in the gluon fusion ($gg \to \tau\bar{\tau}$) and the top-quark associated processes ($gg \to t\bar{t} + \tau\bar{\tau}$)

[38], Generic 2HDM (G2HDM, type-III 2HDM) [39,40], axion-like particle (ALP) [41], NMSSM [42] and so on.[3] If one takes a G2HDM as an illustrative model, the oblique corrections and the LHC constraint on a charged scalar [43,44] do not allow to set both H and A masses around 100 GeV for the $\tau\bar{\tau}$ excess. In this paper we do not discuss the detailed setup and consider the two cases that either H or A resides around 100 GeV. We comment on the other couplings except for the effective Lagrangian in Eq. (4), which exist in the UV completed models in general. We suppose only that the gluon-fusion of ϕ is dominated in the top-quark loop contribution, which would be correct when the coupling to the bottom quark is not comparable to the top one. Then, a correlation between two cross sections, $\sigma(pp \to gg \to \phi \to \tau\bar{\tau})$ and $\sigma(pp \to t\bar{t}+\phi \to t\bar{t}+\tau\bar{\tau})$, becomes robust and is independent of the ϕ's decay modes with the other interactions not presented in Eq. (4) (including dark sectors).

2.1 CP-even scalar scenario

First, we consider the case that the resonance reported by the CMS collaboration is a CP-even scalar H. The gluon fusion production cross section of H at $\sqrt{s} = 13$ TeV is predicted as follows

$$\sigma(pp \to gg \to H) = 87.2\,(\rho^H_{tt})^2 \text{ pb} \quad \text{for } m_H = 95\,\text{GeV}, \tag{5}$$

$$\sigma(pp \to gg \to H) = 79.5\,(\rho^H_{tt})^2 \text{ pb} \quad \text{for } m_H = 100\,\text{GeV}, \tag{6}$$

which are evaluated by `SusHi v1.7.0` [45,46] at next-to-next-to leading order (NNLO).[4] The di-tau excess in Eqs. (1) and (2) can be accommodated by

$$\rho^H_{tt}\sqrt{\text{BR}(H \to \tau\bar{\tau})} = 0.30 \pm 0.07 \quad \text{for } m_H = 95\,\text{GeV}, \tag{7}$$

$$\rho^H_{tt}\sqrt{\text{BR}(H \to \tau\bar{\tau})} = 0.27 \pm 0.05 \quad \text{for } m_H = 100\,\text{GeV}. \tag{8}$$

We find that ρ^H_{tt} is sizable to explain the excess: $\rho^H_{tt} \gtrsim 0.22$.

The ρ^H_{tt} interaction also contributes to the production of ϕ in association with two top quarks, as shown in the middle and right diagrams in Fig. 1. The production cross section at $\sqrt{s} = 13$ TeV is obtained as

$$\sigma(pp \to t\bar{t} + H) = 1.07\,(\rho^H_{tt})^2 \text{ pb} \quad \text{for } m_H = 95\,\text{GeV}, \tag{9}$$

$$\sigma(pp \to t\bar{t} + H) = 0.94\,(\rho^H_{tt})^2 \text{ pb} \quad \text{for } m_H = 100\,\text{GeV}, \tag{10}$$

at next-to leading order (NLO). Here, we evaluate the production cross section at the leading order by `MadGraph5_aMC@NLO` [47] and multiply the NLO K factor of 1.29 for simplicity [48].

Combining the above results, the explanation of the excess predicts a sizable cross section of $pp \to t\bar{t}H \to t\bar{t} + \tau\bar{\tau}$:

$$\sigma(pp \to t\bar{t} + H) \times \text{BR}(H \to \tau\bar{\tau}) = [0.056, 0.094, 0.14] \text{ pb} \quad \text{for } m_H = 95\,\text{GeV}, \tag{11}$$

$$\sigma(pp \to t\bar{t} + H) \times \text{BR}(H \to \tau\bar{\tau}) = [0.045, 0.069, 0.097] \text{ pb} \quad \text{for } m_H = 100\,\text{GeV}, \tag{12}$$

where numbers in parentheses indicate the 1σ range with its central value.

The top-associated production cross section of the SM Higgs boson has been measured with 79.8 fb^{-1} of the Run 2 data [49]: $\sigma(pp \to t\bar{t}+h) = 0.67 \pm 0.14$ pb. This is consistent with the SM prediction, $\sigma(pp \to t\bar{t}+h)_{\text{SM}} = 0.51$ pb. Combining the subsequent decay branching ratio of $\text{BR}(h \to \tau\bar{\tau})_{\text{SM}} \sim 6\%$, $\sigma(pp \to t\bar{t}+h)_{\text{SM}} \times \text{BR}(h \to \tau\bar{\tau})_{\text{SM}} \simeq 0.03$ pb is derived in the SM, and thus the predicted cross section of H is larger than the SM Higgs by a factor of approximately three.

We comment on the top-associated Z production cross section. It has been measured based on the full Run 2

[3] As a specific model example, one can consider the flavor-aligned 2HDM which can approximately reproduce the Lagrangian in Eq. (4) with $\xi_d = 0$, $\xi_\ell = \mathcal{O}(0.1)$ and $\xi_u = \mathcal{O}(0.1)$.

[4] It is noted that the next-to-NNLO (N^{3}LO) correction increases the cross section up to 3%.

data [50]; $\sigma(pp \to t\bar{t} + Z) = 0.99 \pm 0.09\,\text{pb}$.[5] This result is also consistent with the SM prediction, $\sigma(pp \to t\bar{t} + Z)_{\text{SM}} = 0.84^{+0.09}_{-0.10}\,\text{pb}$ at NLO QCD and EW accuracy [51]. Since $\text{BR}(Z \to \ell\bar{\ell})$ is about 3%, we obtain $\sigma(pp \to t\bar{t} + Z) \times \text{BR}(Z \to \tau\bar{\tau}) \simeq 0.03\,\text{pb}$, that is comparable to the top-associated production of h.

2.2 CP-odd scalar scenario

Next, we consider the CP-odd scalar A interpretation. The analysis in Sect. 2.1 is applied to this case, replacing H with A. The sizes of the cross sections are, however, different because of the couplings in Eq. (4), so that the predictions are totally different.

The gluon fusion cross section of A at $\sqrt{s} = 13\,\text{TeV}$ is

$$\sigma(pp \to gg \to A) = 201.7\,(\rho^A_{tt})^2\,\text{pb} \quad \text{for } m_A = 95\,\text{GeV}, \tag{13}$$

$$\sigma(pp \to gg \to A) = 184.4\,(\rho^A_{tt})^2\,\text{pb} \quad \text{for } m_A = 100\,\text{GeV}, \tag{14}$$

at NNLO [45,46]. Assuming $\rho^H_{tt} = \rho^A_{tt}$, these predictions are twice as large as them in the H case due to the different γ_5 structure in the top-quark loop. The di-tau excess in Eqs. (1) and (2) can be accommodated by

$$\rho^A_{tt}\sqrt{\text{BR}(A \to \tau\bar{\tau})} = 0.20 \pm 0.04 \quad \text{for } m_A = 95\,\text{GeV}, \tag{15}$$

$$\rho^A_{tt}\sqrt{\text{BR}(A \to \tau\bar{\tau})} = 0.18 \pm 0.03 \quad \text{for } m_A = 100\,\text{GeV}. \tag{16}$$

The production cross section of the top-associated production is

$$\sigma(pp \to t\bar{t} + A) = 0.30\,(\rho^A_{tt})^2\,\text{pb} \quad \text{for } m_A = 95\,\text{GeV}, \tag{17}$$

$$\sigma(pp \to t\bar{t} + A) = 0.29\,(\rho^A_{tt})^2\,\text{pb} \quad \text{for } m_A = 100\,\text{GeV}, \tag{18}$$

where the same NLO K factor as in the CP-even scalar production is assumed [52]. In Ref. [52], it has been shown that the NLO K-factors are almost independent of the CP-even/odd and the mass. In contrast to the gluon fusion cross section, the results are three times as small as them in the H case when $\rho^H_{tt} = \rho^A_{tt}$, as shown in Eqs. (9) and (10). This is again originated from the γ_5 structure. There is a destructive interference between the contribution of the middle diagram and that of the right diagram in Fig. 1 [52–54].

As a result, the cross section of $pp \to t\bar{t} + A \to t\bar{t} + \tau\bar{\tau}$, that is consistent with the di-tau excess, is predicted to be smaller than that of the H case:

$$\sigma(pp \to t\bar{t} + A) \times \text{BR}(A \to \tau\bar{\tau}) = [0.007, 0.011, 0.017]\,\text{pb} \quad \text{for } m_A = 95\,\text{GeV}, \tag{19}$$

$$\sigma(pp \to t\bar{t} + A) \times \text{BR}(A \to \tau\bar{\tau}) = [0.005, 0.009, 0.013]\,\text{pb} \quad \text{for } m_A = 100\,\text{GeV}. \tag{20}$$

It is also known that the angular correlation and transverse momentum distributions of $pp \to t\bar{t} + A$ are different from $pp \to t\bar{t} + H$ due to the presence of γ_5 in Eq. (4) [54].

3 Comparisons to the ATLAS data

In this section, we compare the CMS di-tau excesses in Eqs. (1) and (2) to the ATLAS results that involve $\tau\bar{\tau}$ in the final states. Since the range of the ATLAS data set for the exotic particle search decaying to $\tau\bar{\tau}$ is $m_{\tau\tau} \geq 200\,\text{GeV}$ [10], the 95–100 GeV region has not been covered. Instead, we utilize the ATLAS Run 2 full data for the $h \to \tau\bar{\tau}$ decay channel where h is the SM Higgs boson [55]. The $h \to \tau\bar{\tau}$ and $Z \to \tau\bar{\tau}$ events have been carefully studied by using the several production processes. Therefore the additional narrow resonance ϕ that decays to $\tau\bar{\tau}$ can also be probed. In the following, we analyze the data in the *boosted* $\tau_\text{h}\tau_\text{h}$ and $tt(0\ell) + \tau_\text{h}\tau_\text{h}$ *categories* [55], where τ_h denotes τ that decays hadronically.

3.1 Boosted $\tau\bar{\tau}$ search

The boost categories defined in Ref. [55] consist of the events that fail to meet the criteria of the vector-boson fusion (VBF), vector-boson associated production (VH), and a pair of top-quark associated production. The events have high-p_T (boosted) Higgs candidates. The more than 70% events, actually, come from the gluon fusion with large Higgs boson transverse momentum in the analysis of Ref. [55]. Hence, the ATLAS data in this category should be a good comparison to the CMS di-tau excess. We use the result in the *boost_2 category* corresponding to $200 < p_\text{T}^{\tau\tau} < 300\,\text{GeV}$ in Ref. [55].[6]

Using the the narrow width approximation, we define a signal strength for the gluon fusion of ϕ,

$$\mu_\phi(\tau\bar{\tau}) \equiv \frac{\sigma(pp \to gg \to \phi) \times \text{BR}(\phi \to \tau\bar{\tau})}{\sigma(pp \to gg \to h)_{\text{SM}} \times \text{BR}(h \to \tau\bar{\tau})_{\text{SM}}}, \tag{21}$$

[5] The cross section of $\sigma(pp \to t\bar{t} + Z)$ has been measured in $Z \to \ell\bar{\ell}$ with $\ell = e$ and μ channels.

[6] We found that the data in *boost_3 category* corresponding to $p_\text{T}^{\tau\tau} > 300\,\text{GeV}$ is less sensitive in the following analysis due to the small amount of statistics.

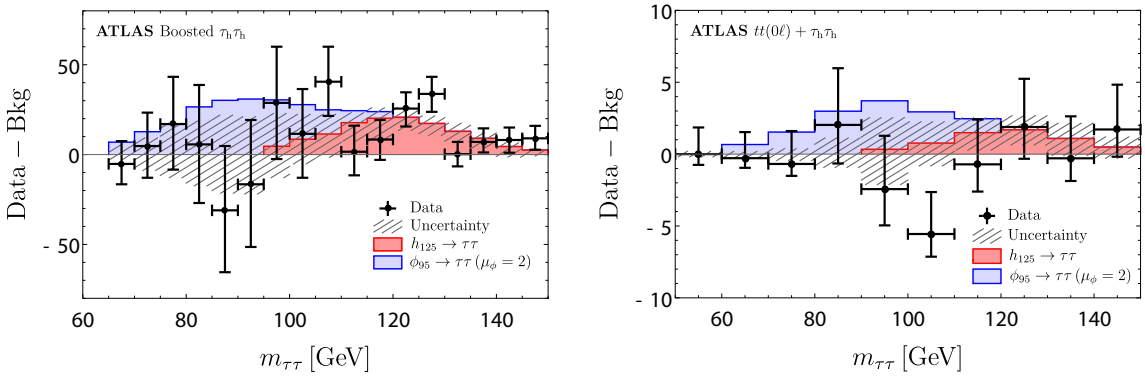

Fig. 2 The histograms of the additional resonance ϕ (blue) and SM Higgs (red) event shapes are shown with the experimental data (cross) and their uncertainties (dashed band). The left panel is for the boosted $\tau_h\tau_h$ and the right panel is the $tt(0\ell) + \tau_h\tau_h$ categories, respectively. The signal normalization is assumed to be $\mu_\phi = 2$, and $m_\phi = 95\,\text{GeV}$ are set for the mass. See the text for details

where the denominator is values of the 125 GeV SM Higgs. In the left panel of Fig. 2, an expected histogram of the ϕ with $m_\phi = 95\,\text{GeV}$ and $\mu_\phi(\tau\bar{\tau}) = 2$ is shown by the blue shaded region. Here the SM Background (Bkg), except for the SM Higgs boson, is subtracted from the data which corresponds to the bottom-left panel of Fig. 20 (*boost_2 category*) of Ref. [55]. Note that the SM Higgs histogram (red shaded region) stands for $pp \to h \to \tau\bar{\tau}$ and is scaled by $1/0.93$ from the original figure.[7] The $0.93\,(^{+0.13}_{-0.12})$ is a global fit result of the signal strength of $pp \to h \to \tau\bar{\tau}$ [55]. The dashed band represents the total uncertainty of the SM Bkg. It is shown that there is a huge uncertainty around $m_{\tau\tau} = 80$–$100\,\text{GeV}$, which comes from the DY (boosted) Z-boson production.

By using a χ^2 test which will be explicitly defined in the next section, we set 95% confidence level (CL) upper limits on the signal strength,

$$\mu_\phi(\tau\bar{\tau}) < 3.78 \quad \text{for } m_\phi = 95\,\text{GeV}, \tag{22}$$

$$\mu_\phi(\tau\bar{\tau}) < 3.61 \quad \text{for } m_\phi = 100\,\text{GeV}, \tag{23}$$

or equivalently, the upper limits on the production cross sections,

$$\sigma(gg \to \phi) \times \text{BR}(\phi \to \tau\bar{\tau}) < 11.5\,\text{pb} \quad \text{for } m_\phi = 95\,\text{GeV}, \tag{24}$$

$$\sigma(gg \to \phi) \times \text{BR}(\phi \to \tau\bar{\tau}) < 11.0\,\text{pb} \quad \text{for } m_\phi = 100\,\text{GeV}. \tag{25}$$

We find that the ATLAS data in the boosted $\tau_h\tau_h$ category are consistent with the CMS di-tau excess in Eqs. (1) and (2) even if the upper edge of the 1σ is considered.

[7] We also subtract the non gluon-fusion contributions according as Table 11 of Ref. [55] to construct the histogram of ϕ.

3.2 $t\bar{t} + \tau\bar{\tau}$ search

In this section, we compare the CMS di-tau excess with the ATLAS data in the $tt(0\ell) + \tau_h\tau_h$ category [55]. Due to the limited statistics, the ATLAS collaboration has not performed a serious top reconstruction, but just imposed either six jets including at least one b-tagged jet or five jets including at least two b-tagged jets for the event selection.

As mentioned in Sect. 1, the additional $t\bar{t}$ requirement is expected to improve the sensitivity to probe the new resonance, because the huge DY Z-boson Bkg can be vetoed and the production cross sections of $t\bar{t} + \{h, Z, \phi\} \to t\bar{t} + \tau\bar{\tau}$ are of the same size. However, since the top-quark tagging has not been seriously imposed in this ATLAS data, the SM Bkg is still dominated by the DY process ($pp \to Z + 5 - 6\,\text{QCD jets}$), and still large Bkg remains even in the signal region ($m_{\tau\tau} \simeq 125\,\text{GeV}$), as one can see in Fig. 11 of Ref. [55]. The region of interest in this paper is $m_{\tau\tau} = 95$–$100\,\text{GeV}$, and hence we have the large Bkg from $Z \to \tau\bar{\tau}$. Nonetheless, we use this result to derive the current experimental limit on the new resonance production. It is naively expected that a severe top-quark tagging algorithm (by the mass reconstruction) improves the sensitivity.

Since experimental analyses have used the boosted decision tree (BDT) techniques, it is difficult to access the detailed information about the final kinematic cuts. Instead, we utilize the data in *ttH_1 category*, corresponding to the right panel of Fig. 11 of Ref. [55], where the $t\bar{t}h$ events are optimised to be enhanced over Z and $t\bar{t}$ Bkg events by the BDT. In the plot, (data yields) − (SM Bkg except for the SM Higgs) is shown ($N_{\text{ob}} \pm \Delta N_{\text{ob}}$), as well as uncertainty of the total SM Bkg ($\pm\Delta N_{\text{Bkg}}$) and the SM Higgs histogram (N_h). From this figure, we estimate the sensitivity to probe the new resonance, supposing that the $m_{\tau\tau}$ distribution of $t\bar{t} + \phi \to t\bar{t} + \tau\bar{\tau}$ under the BDT is similar to the SM Higgs.

Table 1 The 95% CL upper limits on the signal strengths (μ_ϕ) and the production cross sections for $m_\phi = 95,\ 100,\ 105\,\text{GeV}$ are summarized. These limits are obtained from the ATLAS Run 2 full data [55] in the boosted $\tau\bar{\tau}$ (boost_2 category) and $t\bar{t}+\tau\bar{\tau}$ ($tt(0\ell)+\tau_h\tau_h$ category) searches, via the χ^2 test defined in Eq. (27)

	$m_\phi = 95\,\text{GeV}$	$m_\phi = 100\,\text{GeV}$	$m_\phi = 105\,\text{GeV}$
$\mu_\phi(\tau\bar{\tau})$	< 3.78	< 3.61	< 2.00
$\sigma(gg\to\phi)\times\text{BR}(\phi\to\tau\bar{\tau})$	$< 11.5\,\text{pb}$	$< 11.0\,\text{pb}$	$< 6.08\,\text{pb}$
$\mu_\phi(t\bar{t}+\tau\bar{\tau})$	< 1.56	–	< 1.10
$\sigma(pp\to t\bar{t}+\phi)\times\text{BR}(\phi\to\tau\bar{\tau})$	$< 0.050\,\text{pb}$	–	$< 0.035\,\text{pb}$

Similar to the previous section, we define a signal strength for the top-associated production of ϕ,

$$\mu_\phi(t\bar{t}+\tau\bar{\tau}) \equiv \frac{\sigma(pp\to t\bar{t}+\phi)\times\text{BR}(\phi\to\tau\bar{\tau})}{\sigma(pp\to t\bar{t}+h)_{\text{SM}}\times\text{BR}(h\to\tau\bar{\tau})_{\text{SM}}}. \tag{26}$$

In the right panel of Fig. 2, an expected histogram of ϕ with $m_\phi = 95\,\text{GeV}$ and $\mu_\phi(t\bar{t}+\tau\bar{\tau}) = 2$ is shown by the blue shaded region. Since the each bin width in the data is 10 GeV, we simply shift the distribution of the SM Higgs histogram by three bins to obtain the distribution of $m_\phi = 95\,\text{GeV}$.[8] Since the width of the SM Higgs histogram stems from the experimental resolution, it is expected that the width of the histogram of ϕ is roughly of the same size as the SM Higgs. Moreover, if the resolution is proportional to the value of $m_{\tau\tau}$, the histogram of ϕ becomes sharpened. Therefore, we just rescale the SM Higgs histogram to conservatively predict the ϕ contribution. We represent the histogram of ϕ by $N_\phi(\mu_\phi)$. Again, the SM Higgs histogram (red shaded region) is scaled by $1/0.93$ from the original one.

We perform the following χ^2 test,

$$\chi^2(\mu_\phi) = \max\left[\chi_i^2(\mu_\phi)\right] \quad \text{and} \quad \chi_i^2(\mu_\phi) = \sum_{j=i}^{i+2} \frac{\left[N_{\text{ob}}^j - N_h^j - N_\phi(\mu_\phi)^j\right]^2}{(\Delta N_{\text{ob}}^j)^2 + (\Delta N_{\text{Bkg}}^j)^2}, \tag{27}$$

where i and j are indices of each bin. Note that since correlations between the data in each bin are not available in Ref. [55], we discard them for simplicity. Due to the finite experimental resolution for the $m_{\tau\tau}$ distribution, judging based on the single bin data is too aggressive. Here, we use at least 3 contiguous bins for each $\chi_i^2(\mu_\phi)$ evaluation.[9] The criterion for setting the upper limit on μ_ϕ is $\chi^2(\mu_\phi) < \chi^2_{3\text{dof},95\%} \simeq 7.82$.

As a validation of this χ^2 test, we compare the upper limit on the SM Higgs production cross section in the ttH_1 category. We obtain the 95% CL upper limit for the Higgs boson cross section,

$$\mu_h = \frac{\sigma(pp\to t\bar{t}+h)\times\text{BR}(h\to\tau\bar{\tau})}{\sigma(pp\to t\bar{t}+h)_{\text{SM}}\times\text{BR}(h\to\tau\bar{\tau})_{\text{SM}}} \le 2.65, \tag{28}$$

while $\mu_h \lesssim 2.96$ ($\mu_h = 1.02^{+0.97}_{-0.81}$) has been set in Ref. [55]. It is found that the χ^2 test in Eq. (27) gives a slightly severe limit. This could be attributed to the following reasons; This χ^2 test does not include the theoretical uncertainty of the signal events properly. The total uncertainty (dashed band ΔN_{Bkg}) includes the theoretical uncertainty of $\mu_h \simeq 1$ and it should be inflated according as μ_h. Second, when we evaluate the χ_i^2 value for at least not 3 but 4 contiguous bins, the resultant limit is weakened by 5–10%. Therefore, we decide to weaken the obtained upper limit on μ_ϕ by 10% to be conservative test. In this prescription, we obtain $\mu_h < 2.92$.

Using the χ^2 test, we set the 95% CL upper limit on the signal strength,

$$\mu_\phi(t\bar{t}+\tau\bar{\tau}) < 1.56 \quad \text{for } m_\phi = 95\,\text{GeV}, \tag{29}$$

or equivalently,

$$\sigma(pp\to t\bar{t}+\phi)\times\text{BR}(\phi\to\tau\bar{\tau}) < 0.050\,\text{pb} \quad \text{for } m_\phi = 95\,\text{GeV}. \tag{30}$$

It is found that the CP-even scalar H interpretation on the CMS di-tau is excluded by the ATLAS $t\bar{t}+\tau\bar{\tau}$ search, while the CP-odd A one is consistent with the ATLAS (see Eqs. (11) and (19)). Note that due to the fixed bin width, we can not perform the same analysis for the $m_\phi = 100\,\text{GeV}$ case.[10] Our results are summarized in Table 1.

Finally, we project the obtained ATLAS limits onto the the minimal setup in Eq. (4). In Fig. 3, we show the ATLAS

[8] See also Sect. 4 for a discussion of this treatment.

[9] We found that χ^2 tests for $\mu_\phi(t\bar{t}+\tau\bar{\tau})$ with 2 contiguous bins give roughly 30% stronger constraints for both $m_\phi = 95$ GeVand 105 GeV, while the analyses using 4 contiguous bins bring 25% and 40% weaker constraints for 95 GeVand 105 GeV, respectively.

[10] We performed the same χ^2 test for $m_\phi = 105\,\text{GeV}$, and the result is $\mu_\phi(t\bar{t}+\tau\bar{\tau}) < 1.10$, which is not far from Eq. (29). This result implies that the upper limit for $m_\phi = 100\,\text{GeV}$ would be the same size as the $m_\phi = 95\,\text{GeV}$ case.

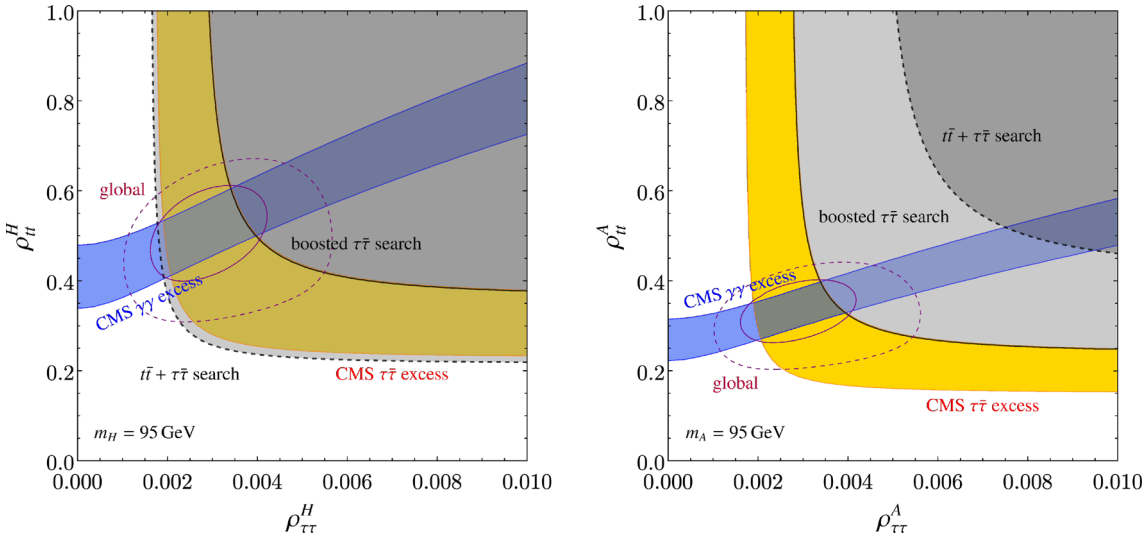

Fig. 3 The obtained ATLAS 95% CL limits are shown on a $\rho_{\tau\tau}$–ρ_{tt} plane (see Table 1). The gray shaded regions surrounded by the solid and dashed lines are excluded by the ATLAS boosted $\tau\bar{\tau}$ and $t\bar{t}+\tau\bar{\tau}$ searches, respectively. The left panel is for the CP-even (H) case and the right one is for the CP-odd (A). The CMS di-tau and di-photon excesses can be explained at the 1σ level in the yellow and blue regions, respectively. The global fits at the 1σ (2σ) level are shown by the purple solid (dashed) circles. The scalar boson mass is set to be 95 GeV

limits from the data in the boosted $\tau\bar{\tau}$ and $t\bar{t}+\tau\bar{\tau}$ searches by the gray shaded regions surrounded by the solid and dashed lines, respectively. The CP-even (odd) scalar with $m_{H(A)} = 95$ GeV is considered in the left (right) panel. The CMS di-tau excess in Eq. (1) can be explained in the yellow region. For the branching ratio, we calculate $H(A) \to \tau\bar{\tau}$ at the tree level and gg, $\gamma\gamma$ and $Z\gamma$ at the one-loop level [56] for the decay channels. Furthermore, the aforementioned CMS di-photon excess can be explained in the blue region corresponding to [13,23]

$$\sigma(gg \to \phi) \times \mathrm{BR}(\phi \to \gamma\gamma) = 0.058 \pm 0.019\,\mathrm{pb}, \qquad (31)$$

where the `SusHi` and Ref. [57] are used for the 95 GeV SM-like Higgs value. It is clearly shown that an interesting parameter region that can explain both di-tau and di-photon excesses is almost excluded in the CP-even scalar case. Note that although the results on Fig. 3 assume the minimal setup in Eq. (4), the statement that the anomaly-driven parameter region is excluded in the CP-even scalar case is independent of the effective Lagrangian as long as the gluon-fusion is dominated in the top-quark contribution. Additional interactions including dark sectors reduce only $\mathrm{BR}(\phi \to \tau\bar{\tau})$. This effect shifts the results to the upper-right direction on Fig. 3, but the relative positions do not change.

3.3 Comment on $t\bar{t}+\gamma\gamma$ search

Motivated by the CMS di-photon excess in Eq. (31), we point out that the above procedure can be repeated to estimate the upper limit on $\sigma(pp \to t\bar{t}+\phi) \times \mathrm{BR}(\phi \to \gamma\gamma)$ by analysing $pp \to t\bar{t}+h \to t\bar{t}+\gamma\gamma$ process. This process must be cleaner than the $pp \to t\bar{t}+\{h, Z\} \to t\bar{t}+\tau\bar{\tau}$. This is because the $Z \to \gamma\gamma$ decay is forbidden (the Landau–Yang theorem [58,59]) so much smaller SM Bkg is expected around $m_{\gamma\gamma} \sim 90$ GeV.[11] Furthermore, $\sigma(pp \to t\bar{t}+\phi) \times \mathrm{BR}(\phi \to \gamma\gamma)$ is expected to be the same size as the $\sigma(pp \to t\bar{t}+h)_{\mathrm{SM}} \times \mathrm{BR}(h \to \gamma\gamma)_{\mathrm{SM}}$. Therefore, the search for the additional resonance in $pp \to t\bar{t}+\gamma\gamma$ is promising.

Indeed, such a check has been implicitly done in the CMS collaboration [13]. However, we could not find any results of direct searches for $pp \to t\bar{t}+\gamma\gamma$ in a region of $m_{\gamma\gamma} \leq 105$ GeV [49,60,61] (see, e.g., Fig. 2 of Ref. [60]). Therefore, we would like to suggest an experimental analysis of the $pp \to t\bar{t}+\gamma\gamma$ process with the low-mass region to probe the additional resonance.

4 Summary and discussion

Due to the nature of the high-energy proton collider and its harsh hadron activity, it is difficult to probe weakly interacting colorless new particles below $\mathcal{O}(100)$ GeV mass region. Very recently, the CMS collaboration has reported a di-tau excess with a local significance of 2.6–3.1σ around $m_{\tau\tau} =$ 95–100 GeV. This excess can be interpreted as an additional scalar boson ϕ produced via the gluon-fusion process. Interestingly, in the same mass region, two other excesses have been reported; a di-photon excess by the CMS collaboration and an excess in $e^+e^- \to Zb\bar{b}$ from the LEP experiment.

[11] Still, there is a doubly photon-misidentified Bkg from $Z \to e^+e^-$ [13].

In this paper, we focus on the CMS di-tau excess. This excess can be explained by the light scalar ϕ which couples with the top and τ in the minimal setup. First, we found that the minimal scalar model is still consistent with the ATLAS result for the similar boosted $\tau\bar{\tau}$ search, where a huge SM Bkg comes from the Z-boson DY production. Second, we point out that the minimal scalar model predicts the inevitable correlation with the top-quark associated process ($gg \to t\bar{t} + \tau\bar{\tau}$), see the Feynman diagrams in Fig. 1. Moreover, a requirement of an additional top-quark pair in the final state suppresses the huge Z-boson DY Bkg, so that the experimental sensitivity to probe ϕ is certainly better compared to the boosted $\tau\bar{\tau}$ search around $m_{\tau\tau} = 95$–$100\,\text{GeV}$, although the statistics are limited.

Based on the ATLAS data available in Ref. [55], we obtain the 95% CL upper limits on the gluon-fusion and top-associated production cross sections in the minimal setup, which are summarized in Table 1. One of important points is that the limits depend on the CP eigenstate of ϕ, i.e., whether ϕ is CP-even (H) or CP-odd (A). We point out that the gluon-fusion production cross section is twice larger in the A case, while the top-associated production cross section is three times larger in the H case including the QCD higher-order corrections. This difference is caused by the γ_5 structure in the Yukawa interaction. As the result, it is found that the H interpretation on the di-tau excess is excluded by the ATLAS $t\bar{t} + \tau\bar{\tau}$ search, while the A case is allowed, see Fig. 3. The available ATLAS data (the $tt(0\ell) + \tau_h\tau_h$ category) is pure hadronic final states. We also hope the ATLAS collaboration to stop categorizing and to combine both leptonic [62,63] and hadronic decay modes [55] to increase the sensitivity to probe a possible new particle. The similar analysis could also be applied in $t\bar{t} + \gamma\gamma$ search to probe a possible light resonance that can accommodate the CMS di-photon excess.

Note that the LEP $b\bar{b}$ excess implies that ϕ is the CP-even state (H) because the Z-boson-associated A production vanishes. Therefore, once the $b\bar{b}$ excess is involved seriously, the CP symmetry must be violated in the scalar model. Such CP-violating parameters (Yukawa or scalar self interactions) would induce the electron electric dipole moment at two-loop level (e.g., Ref. [64]). Furthermore, a search for $t\bar{t} + b\bar{b}$ signature would be interesting in light of the $b\bar{b}$ excess. Although Fig. 12 of Ref. [65] would be helpful to check the $b\bar{b}$ excess, the measurement suffers from the QCD jets. The more statistics and dedicated study are necessary to make a clear conclusion.

An additional vector particle (A') would be also a possibility for the CMS di-tau excess. The simplest possibility is the hidden-photon model [66,67]. The production of A' is the DY process and the decay branching ratio is fixed [$\text{BR}(A' \to \tau\bar{\tau}) \simeq 15\%$] [68]. Currently there is no direct experimental bound on the A' production with mass region of around 90 GeV at the LHC [69]. Instead, an indirect bound comes from measurements of the EW precision observables at the LEP and Tevatron experiments [70]. It is, however, beyond the scope of this paper to examine whether the A' interpretation is allowed.

We also comment on our prescription for the χ^2 test in Eq. (27). Our prescription is intuitive and does not rely on realistic Monte-Carlo simulations. Necessary cut information for the detailed analysis is not available from the experimental papers because the BDT algorithm is adopted. Our prescription may receive additional effects from the BDT, since the BDT variables include the sub-leading p_T^τ and missing transverse momentum.

Since the current ATLAS data is consistent with the CMS di-tau excess if a light CP-odd scalar is introduced, it is nice to consider specific new physics models. A light CP-odd scalar emerges as a pseudo-Nambu–Goldstone (NG) boson which comes from the spontaneous symmetry breaking of some global symmetries. Such a mass of the pseudo-NG boson does not lead to an additional fine-tuning problem.

Within the G2HDM, additional scalars appear in the same mass scale with moderate mass differences of $\mathcal{O}(\text{VEV})$ (see, Ref. [71] for instance). It is possible to predict the lighter CP-odd scalar in general. Nevertheless the mass degenerated setup, where only ρ_{tt} and $\rho_{\tau\tau}$ are assumed to be nonzero, is not compatible with the direct search for the charged scalar in $pp \to tb + H^\pm \to tb + \tau\nu$ or tb [43,44]. Therefore the heavier charged scalar is necessary while keeping the CP-odd scalar mass to be around 95 GeV.[12] Another possible solution to this dilemma is to put the additional coupling and open up a new decay mode of a charged scalar. However, additional Yukawa couplings could also contribute to the scalar production and suffers from the direct searches. The weakest constrained Yukawa coupling is a top-charm flavor violating coupling, ρ_{tc}, where top quark is a left handed and charm quark is right handed. Since the top mass is heavier than 100 GeV, the coupling does not reduce the $\text{BR}(\phi \to \tau\bar{\tau})$. On the other hand the $SU(2)_L$ rotation generates $H^- \to b\bar{c}$ decay when ρ_{tc} is not vanishing. It is recently pointed out that low-mass di-bottom jets would be sensitive to this coupling depending on the mass [72]. It is worthwhile to comment that the non-zero product of ρ_{tc} and $\rho_{\tau\tau}$ can enhance $R_{D^{(*)}} = \text{BR}(\bar{B} \to D^{(*)}\tau\bar{\nu})/\text{BR}(\bar{B} \to D^{(*)}\ell\bar{\nu})$, where $\ell = e,\ \mu$ and the 3–4σ discrepancy is reported [73,74], consistently with the B_c-meson lifetime [75].[13] The non-zero ρ_{tc} with the large mass difference between neutral scalars induces the same sign top signal [77]. This is also interesting as well as the search for a light scalar in the double-scalar

[12] The mass degeneracy of a heavier CP-even scalar and a charged scalar is required to satisfy the constraint from the electroweak precision test.

[13] For $m_{H^-} \geq 400\,\text{GeV}$, $\tau\nu$ resonance searches exclude the interpretation [76].

production at the LHC [78]. The more quantitative and dedicated study is beyond this paper and will be given elsewhere.

Acknowledgements S.I. would like to thank Shigeki Hirose, Yuta Takahashi, Ulrich Nierste, Andreas Crivellin, and Hantian Zhang for fruitful comments and valuable discussion. T.K. thanks Junji Hisano, Kazuhiro Tobe, and Nodoka Yamanaka for useful discussion. The work of S.I. is supported by the Deutsche Forschungsgemeinschaft (DFG, German Research Foundation) under Grant 396021762-TRR 257. T.K. is supported by the Grant-in-Aid for Early-Career Scientists (No. 19K14706) from the Ministry of Education, Culture, Sports, Science, and Technology (MEXT), Japan. The work of Y.O. is supported by Grant-in-Aid for Scientific research from the MEXT, Japan, No. 19K03867. This work is also supported by the Japan Society for the Promotion of Science (JSPS) Core-to-Core Program, No. JPJSCCA20200002.

Data Availability Statement This manuscript has no associated data or the data will not be deposited. [Authors' comment: Data sharing is not applicable to this article as no new data were created or analyzed in this study.]

Funded by SCOAP[3]. SCOAP[3] supports the goals of the International Year of Basic Sciences for Sustainable Development.

References

1. ATLAS Collaboration, Search for chargino–neutralino pair production in final states with three leptons and missing transverse momentum in $\sqrt{s} = 13$ TeV pp collisions with the ATLAS detector. Eur. Phys. J. C **81**, 1118 (2021). https://doi.org/10.1140/epjc/s10052-021-09749-7. arXiv:2106.01676
2. ATLAS Collaboration, Search for long-lived charginos based on a disappearing-track signature using 136 fb^{-1} of pp collisions at $\sqrt{s}$ = 13 TeV with the ATLAS detector. Eur. Phys. J. C **82**, 606 (2022). https://doi.org/10.1140/epjc/s10052-022-10489-5. arXiv:2201.02472
3. CMS Collaboration, Searches for additional Higgs bosons and vector leptoquarks in $\tau\tau$ final states in proton–proton collisions at $\sqrt{s} = 13$ TeV. http://cds.cern.ch/record/2803739
4. CMS Collaboration, Search for Neutral MSSM Higgs bosons decaying to tau pairs in pp collisions at $\sqrt{s} = 7$ TeV. Phys. Rev. Lett. **106**, 231801 (2011). https://doi.org/10.1103/PhysRevLett.106.231801. arXiv:1104.1619
5. ATLAS Collaboration, Search for the neutral Higgs bosons of the minimal supersymmetric standard model in pp collisions at $\sqrt{s} =$ 7 TeV with the ATLAS detector. JHEP **02**, 095 (2013). https://doi.org/10.1007/JHEP02(2013)095. arXiv:1211.6956
6. ATLAS Collaboration, Search for neutral Higgs bosons of the minimal supersymmetric standard model in pp collisions at $\sqrt{s} = 8$ TeV with the ATLAS detector. JHEP **11**, 056 (2014). https://doi.org/10.1007/JHEP11(2014)056. arXiv:1409.6064
7. ATLAS Collaboration, Search for Minimal Supersymmetric Standard Model Higgs bosons H/A and for a Z' boson in the $\tau\tau$ final state produced in pp collisions at $\sqrt{s} = 13$ TeV with the ATLAS Detector. Eur. Phys. J. C **76**, 585 (2016). https://doi.org/10.1140/epjc/s10052-016-4400-6. arXiv:1608.00890
8. ATLAS Collaboration, Search for additional heavy neutral Higgs and gauge bosons in the ditau final state produced in 36 fb^{-1} of pp collisions at $\sqrt{s} = 13$ TeV with the ATLAS detector. JHEP **01**, 055 (2018). https://doi.org/10.1007/JHEP01(2018)055. arXiv:1709.07242
9. CMS Collaboration, Search for additional neutral MSSM Higgs bosons in the $\tau\tau$ final state in proton–proton collisions at $\sqrt{s} = 13$ TeV. JHEP **09**, 007 (2018). https://doi.org/10.1007/JHEP09(2018)007. arXiv:1803.06553
10. ATLAS Collaboration, Search for heavy Higgs bosons decaying into two tau leptons with the ATLAS detector using pp collisions at $\sqrt{s} = 13$ TeV. Phys. Rev. Lett. **125**, 051801 (2020). https://doi.org/10.1103/PhysRevLett.125.051801. arXiv:2002.12223
11. C. Anastasiou et al., High precision determination of the gluon fusion Higgs boson cross-section at the LHC. JHEP **05**, 058 (2016). https://doi.org/10.1007/JHEP05(2016)058. arXiv:1602.00695
12. CMS Collaboration, Search for new resonances in the diphoton final state in the mass range between 80 and 115 GeV in pp collisions at $\sqrt{s} = 8$ TeV. https://cds.cern.ch/record/2063739
13. CMS Collaboration, Search for a standard model-like Higgs boson in the mass range between 70 and 110 GeV in the diphoton final state in proton–proton collisions at $\sqrt{s} = 8$ and 13 TeV. Phys. Lett. B **793**, 320–347 (2019). https://doi.org/10.1016/j.physletb.2019.03.064. arXiv:1811.08459
14. ATLAS Collaboration, Search for resonances in the 65 to 110 GeV diphoton invariant mass range using 80 fb^{-1} of pp collisions collected at $\sqrt{s} = 13$ TeV with the ATLAS detector. https://atlas.web.cern.ch/Atlas/GROUPS/PHYSICS/CONFNOTES/ATLAS-CONF-2018-025/
15. S. Heinemeyer, T. Stefaniak, A Higgs Boson at 96 GeV?! PoS **CHARGED2018**, 016 (2019). https://doi.org/10.22323/1.339.0016. arXiv:1812.05864
16. LEP Working Group for Higgs boson searches, ALEPH, DELPHI, L3, OPAL Collaboration, Search for the standard model Higgs boson at LEP. Phys. Lett. B **565**, 61–75 (2003). https://doi.org/10.1016/S0370-2693(03)00614-2. arXiv:hep-ex/0306033
17. P.J. Fox, N. Weiner, Light signals from a lighter Higgs. JHEP **08**, 025 (2018). https://doi.org/10.1007/JHEP08(2018)025. arXiv:1710.07649
18. U. Haisch, A. Malinauskas, Let there be light from a second light Higgs doublet. JHEP **03**, 135 (2018). https://doi.org/10.1007/JHEP03(2018)135. arXiv:1712.06599
19. T. Biekötter, S. Heinemeyer, C. Muñoz, Precise prediction for the Higgs-boson masses in the $\mu\nu$ SSM. Eur. Phys. J. C **78**, 504 (2018). https://doi.org/10.1140/epjc/s10052-018-5978-7. arXiv:1712.07475
20. D. Liu, J. Liu, C.E.M. Wagner, X.-P. Wang, A light Higgs at the LHC and the B-anomalies. JHEP **06**, 150 (2018). https://doi.org/10.1007/JHEP06(2018)150. arXiv:1805.01476
21. F. Domingo, S. Heinemeyer, S. Paßehr, G. Weiglein, Decays of the neutral Higgs bosons into SM fermions and gauge bosons in the $\mathcal{CP}$-violating NMSSM. Eur. Phys. J. C **78**, 942 (2018). https://doi.org/10.1140/epjc/s10052-018-6400-1. arXiv:1807.06322
22. W.G. Hollik, S. Liebler, G. Moortgat-Pick, S. Paßehr, G. Weiglein, Phenomenology of the inflation-inspired NMSSM at the electroweak scale. Eur. Phys. J. C **79**, 75 (2019). https://doi.org/10.1140/epjc/s10052-019-6561-6. arXiv:1809.07371

23. T. Biekötter, M. Chakraborti, S. Heinemeyer, A 96 GeV Higgs boson in the N2HDM. Eur. Phys. J. C **80**, 2 (2020). https://doi.org/10.1140/epjc/s10052-019-7561-2. arXiv:1903.11661
24. J.M. Cline, T. Toma, Pseudo-Goldstone dark matter confronts cosmic ray and collider anomalies. Phys. Rev. D **100**, 035023 (2019). https://doi.org/10.1103/PhysRevD.100.035023. arXiv:1906.02175
25. J. Cao, X. Jia, Y. Yue, H. Zhou, P. Zhu, 96 GeV diphoton excess in seesaw extensions of the natural NMSSM. Phys. Rev. D **101**, 055008 (2020). https://doi.org/10.1103/PhysRevD.101.055008. arXiv:1908.07206
26. J.A. Aguilar-Saavedra, F.R. Joaquim, Multiphoton signals of a (96 GeV?) stealth boson. Eur. Phys. J. C **80**, 403 (2020). https://doi.org/10.1140/epjc/s10052-020-7952-4. arXiv:2002.07697
27. T. Biekötter, M. Chakraborti, S. Heinemeyer, The "96 GeV excess" at the LHC. Int. J. Mod. Phys. A **36**, 2142018 (2021). https://doi.org/10.1142/S0217751X21420185. arXiv:2003.05422
28. T. Biekötter, M.O. Olea-Romacho, Reconciling Higgs physics and pseudo-Nambu-Goldstone dark matter in the S2HDM using a genetic algorithm. JHEP **10**, 215 (2021). https://doi.org/10.1007/JHEP10(2021)215. arXiv:2108.10864
29. T. Biekötter, A. Grohsjean, S. Heinemeyer, C. Schwanenberger, G. Weiglein, Possible indications for new Higgs bosons in the reach of the LHC: N2HDM and NMSSM interpretations. Eur. Phys. J. C **82**, 178 (2022). https://doi.org/10.1140/epjc/s10052-022-10099-1. arXiv:2109.01128
30. S. Heinemeyer, C. Li, F. Lika, G. Moortgat-Pick, S. Paasch, A 96 GeV Higgs boson in the 2HDM plus Singlet. arXiv:2112.11958
31. R. Benbrik, M. Boukidi, S. Moretti, S. Semlali, Explaining the 96 GeV Di-photon anomaly in a generic 2HDM Type-III. Phys. Lett. B **832**, 137245 (2022). https://doi.org/10.1016/j.physletb.2022.137245. arXiv:2204.07470
32. R. Benbrik, M. Boukidi, B. Manaut, W-mass and 96 GeV excess in type-III 2HDM. arXiv:2204.11755
33. T. Biekötter, S. Heinemeyer, G. Weiglein, Mounting evidence for a 95 GeV Higgs boson. JHEP **08**, 201 (2022). https://doi.org/10.1007/JHEP08(2022)201. arXiv:2203.13180
34. T. Biekötter, S. Heinemeyer, G. Weiglein, Excesses in the low-mass Higgs-boson search and the W-boson mass measurement. arXiv:2204.05975
35. K. Kumar, R. Vega-Morales, F. Yu, Effects from new colored states and the Higgs portal on gluon fusion and Higgs decays. Phys. Rev. D **86**, 113002 (2012). https://doi.org/10.1103/PhysRevD.86.113002. arXiv:1205.4244 (Erratum: Phys. Rev. D 87, 119903 (2013))
36. M. Abdullah, M. Dalchenko, T. Kamon, D. Rathjens, A. Thompson, A heavy neutral gauge boson near the Z boson mass pole via third generation fermions at the LHC. Phys. Lett. B **803**, 135326 (2020). https://doi.org/10.1016/j.physletb.2020.135326. arXiv:1912.00102
37. J.M. Campbell, R.K. Ellis, C. Williams, Gluon–gluon contributions to W+ W- production and Higgs interference effects. JHEP **10**, 005 (2011). https://doi.org/10.1007/JHEP10(2011)005. arXiv:1107.5569
38. A. Pich, P. Tuzon, Yukawa alignment in the two-Higgs-doublet model. Phys. Rev. D **80**, 091702 (2009). https://doi.org/10.1103/PhysRevD.80.091702. arXiv:0908.1554
39. G.C. Branco et al., Theory and phenomenology of two-Higgs-doublet models. Phys. Rep. **516**, 1–102 (2012). https://doi.org/10.1016/j.physrep.2012.02.002. arXiv:1106.0034
40. J.M. Cline, Scalar doublet models confront τ and b anomalies. Phys. Rev. D **93**, 075017 (2016). https://doi.org/10.1103/PhysRevD.93.075017. arXiv:1512.02210
41. H. Georgi, D.B. Kaplan, L. Randall, Manifesting the invisible axion at low-energies. Phys. Lett. B **169**, 73–78 (1986). https://doi.org/10.1016/0370-2693(86)90688-X
42. U. Ellwanger, C. Hugonie, A.M. Teixeira, The next-to-minimal supersymmetric standard model. Phys. Rep. **496**, 1–77 (2010). https://doi.org/10.1016/j.physrep.2010.07.001. arXiv:0910.1785
43. ATLAS Collaboration, Search for charged Higgs bosons decaying via $H^{\pm} \to \tau^{\pm}\nu_{\tau}$ in the τ+jets and τ+lepton final states with 36 fb^{-1} of pp collision data recorded at $\sqrt{s} = 13$ TeV with the ATLAS experiment. JHEP **09**, 139 (2018). https://doi.org/10.1007/JHEP09(2018)139. arXiv:1807.07915
44. ATLAS Collaboration, Search for charged Higgs bosons decaying into a top quark and a bottom quark at $\sqrt{s}$ = 13 TeV with the ATLAS detector. JHEP **06**, 145 (2021). https://doi.org/10.1007/JHEP06(2021)145. arXiv:2102.10076
45. R.V. Harlander, S. Liebler, H. Mantler, SusHi: a program for the calculation of Higgs production in gluon fusion and bottom-quark annihilation in the Standard Model and the MSSM. Comput. Phys. Commun. **184**, 1605–1617 (2013). https://doi.org/10.1016/j.cpc.2013.02.006. arXiv:1212.3249
46. R.V. Harlander, S. Liebler, H. Mantler, SusHi Bento: beyond NNLO and the heavy-top limit. Comput. Phys. Commun. **212**, 239–257 (2017). https://doi.org/10.1016/j.cpc.2016.10.015. arXiv:1605.03190
47. J. Alwall et al., The automated computation of tree-level and next-to-leading order differential cross sections, and their matching to parton shower simulations. JHEP **07**, 079 (2014). https://doi.org/10.1007/JHEP07(2014)079. arXiv:1405.0301
48. S. Frixione, V. Hirschi, D. Pagani, H.S. Shao, M. Zaro, Weak corrections to Higgs hadroproduction in association with a top-quark pair. JHEP **09**, 065 (2014). https://doi.org/10.1007/JHEP09(2014)065. arXiv:1407.0823
49. ATLAS Collaboration, Observation of Higgs boson production in association with a top quark pair at the LHC with the ATLAS detector. Phys. Lett. B **784**, 173–191 (2018). https://doi.org/10.1016/j.physletb.2018.07.035. arXiv:1806.00425
50. ATLAS Collaboration, Measurements of the inclusive and differential production cross sections of a top-quark–antiquark pair in association with a Z boson at $\sqrt{s} = 13$ TeV with the ATLAS detector. Eur. Phys. J. C **81**, 737 (2021). https://doi.org/10.1140/epjc/s10052-021-09439-4. arXiv:2103.12603
51. S. Frixione, V. Hirschi, D. Pagani, H.S. Shao, M. Zaro, Electroweak and QCD corrections to top-pair hadroproduction in association with heavy bosons. JHEP **06**, 184 (2015). https://doi.org/10.1007/JHEP06(2015)184. arXiv:1504.03446
52. R. Frederix et al., Scalar and pseudoscalar Higgs production in association with a top-antitop pair. Phys. Lett. B **701**, 427–433 (2011). https://doi.org/10.1016/j.physletb.2011.06.012. arXiv:1104.5613
53. A. Djouadi, The Anatomy of electro-weak symmetry breaking. II. The Higgs bosons in the minimal supersymmetric model. Phys. Rept. **459**, 1–241 (2008). https://doi.org/10.1016/j.physrep.2007.10.005. arXiv:hep-ph/0503173
54. M.J. Dolan, M. Spannowsky, Q. Wang, Z.-H. Yu, Determining the quantum numbers of simplified models in $t\bar{t}X$ production at the LHC. Phys. Rev. D **94**, 015025 (2016). https://doi.org/10.1103/PhysRevD.94.015025. arXiv:1606.00019
55. ATLAS Collaboration, Measurements of Higgs boson production cross-sections in the $H \to \tau^{+}\tau^{-}$ decay channel in pp collisions at $\sqrt{s} = 13$ TeV with the ATLAS detector. JHEP**08**, 175 (2022). https://doi.org/10.1007/JHEP08(2022)175. arXiv:2201.08269. https://www.hepdata.net/record/ins2014187
56. J.F. Gunion, H.E. Haber, G.L. Kane, S. Dawson, The Higgs Hunter's Guide, vol. 80 (2000)
57. A. Denner, S. Heinemeyer, I. Puljak, D. Rebuzzi, M. Spira, Standard model Higgs-boson branching ratios with uncertainties. Eur. Phys. J. C **71**, 1753 (2011). https://doi.org/10.1140/epjc/s10052-011-1753-8. arXiv:1107.5909

58. L.D. Landau, On the angular momentum of a system of two photons. Dokl. Akad. Nauk Ser. Fiz. **60**, 207–209 (1948). https://doi.org/10.1016/B978-0-08-010586-4.50070-5
59. C.-N. Yang, Selection rules for the dematerialization of a particle into two photons. Phys. Rev. **77**, 242–245 (1950). https://doi.org/10.1103/PhysRev.77.242
60. ATLAS Collaboration, CP Properties of Higgs boson interactions with top quarks in the $t\bar{t}H$ and tH processes using $H \to \gamma\gamma$ with the ATLAS Detector. Phys. Rev. Lett. **125**, 061802 (2020). https://doi.org/10.1103/PhysRevLett.125.061802. arXiv:2004.04545
61. C.M.S. Collaboration, Measurements of Higgs boson production cross sections and couplings in the diphoton decay channel at $\sqrt{s}$ = 13 TeV. JHEP **07**, 027 (2021). https://doi.org/10.1007/JHEP07(2021)027. arXiv:2103.06956
62. ATLAS Collaboration, Evidence for the associated production of the Higgs boson and a top quark pair with the ATLAS detector. Phys. Rev. D **97**, 072003 (2018). https://doi.org/10.1103/PhysRevD.97.072003. arXiv:1712.08891
63. ATLAS Collaboration, Analysis of $t\bar{t}H$ and $t\bar{t}W$ production in multilepton final states with the ATLAS detector. https://cds.cern.ch/record/2693930
64. K. Fuyuto, J. Hisano, E. Senaha, Toward verification of electroweak baryogenesis by electric dipole moments. Phys. Lett. B **755**, 491–497 (2016). https://doi.org/10.1016/j.physletb.2016.02.053. arXiv:1510.04485
65. ATLAS Collaboration, Search for the standard model Higgs boson produced in association with top quarks and decaying into a $b\bar{b}$ pair in pp collisions at $\sqrt{s}$ = 13 TeV with the ATLAS detector. Phys. Rev. D **97**, 072016 (2018). https://doi.org/10.1103/PhysRevD.97.072016. arXiv:1712.08895
66. P. Fayet, U-boson production in e+ e- annihilations, psi and upsilon decays, and light dark matter. Phys. Rev. D **75**, 115017 (2007). https://doi.org/10.1103/PhysRevD.75.115017. arXiv:hep-ph/0702176
67. M. Pospelov, Secluded U(1) below the weak scale. Phys. Rev. D **80**, 095002 (2009). https://doi.org/10.1103/PhysRevD.80.095002. arXiv:0811.1030
68. M. Buschmann, J. Kopp, J. Liu, P.A.N. Machado, Lepton jets from radiating dark matter. JHEP **07**, 045 (2015). https://doi.org/10.1007/JHEP07(2015)045. arXiv:1505.07459
69. C.M.S. Collaboration, Search for a narrow resonance lighter than 200 GeV decaying to a pair of muons in proton–proton collisions at $\sqrt{s}$ = TeV. Phys. Rev. Lett. **124**, 131802 (2020). https://doi.org/10.1103/PhysRevLett.124.131802. arXiv:1912.04776
70. D. Curtin, R. Essig, S. Gori, J. Shelton, Illuminating dark photons with high-energy colliders. JHEP **02**, 157 (2015). https://doi.org/10.1007/JHEP02(2015)157. arXiv:1412.0018
71. S. Iguro, K. Tobe, $R(D^{(*)})$ in a general two Higgs doublet model. Nucl. Phys. B **925**, 560–606 (2017). https://doi.org/10.1016/j.nuclphysb.2017.10.014. arXiv:1708.06176
72. S. Iguro, Revival of H- interpretation of RD(*) anomaly and closing low mass window. Phys. Rev. D **105**, 095011 (2022). https://doi.org/10.1103/PhysRevD.105.095011. arXiv:2201.06565
73. Y. Aoki, et al., FLAG Review 2021. arXiv:2111.09849
74. S. Iguro, R. Watanabe, Bayesian fit analysis to full distribution data of $\bar{B} \to D^{(*)} \ell \bar{\nu}$: $|V_{cb}|$ determination and new physics constraints. JHEP **08**, 006 (2020). https://doi.org/10.1007/JHEP08(2020)006. arXiv:2004.10208
75. M. Blanke, S. Iguro, H. Zhang, Towards ruling out the charged Higgs interpretation of the $R_{D^{(*)}}$ anomaly. JHEP **06**, 043 (2022). https://doi.org/10.1007/JHEP06(2022)043. arXiv:2202.10468
76. S. Iguro, Y. Omura, M. Takeuchi, Test of the $R(D^{(*)})$ anomaly at the LHC. Phys. Rev. D **99**, 075013 (2019). https://doi.org/10.1103/PhysRevD.99.075013. arXiv:1810.05843
77. S. Iguro, Y. Omura, Status of the semileptonic B decays and muon g-2 in general 2HDMs with right-handed neutrinos. JHEP **05**, 173 (2018). https://doi.org/10.1007/JHEP05(2018)173. arXiv:1802.01732
78. ATLAS Collaboration, Search for resonant and non-resonant Higgs boson pair production in the $b\bar{b}\tau^+\tau^-$ decay channel using 13 TeV pp collision data from the ATLAS detector. http://cds.cern.ch/record/2777236